

Development and Evaluation of Epoxy-Based Composites Containing NiO, Cr₂O₃, MnO₂, FeB and TiB₂ for Enhanced Neutron Shielding Performance

B. Aygün^{1*} and A. Karabulut²

^{1*}Department of Electronics and Automation, Vocational School, Agri Ibrahim Cecen University, Agri, Turkey

²Department of Physics, Faculty of Science, Ataturk University, 25040, Erzurum, and Agri Ibrahim Cecen University, Agri, Turkey,
akara@atauni.edu.tr

Abstract

Epoxy-based multifunctional composites reinforced with NiO, Cr₂O₃, MnO₂, FeB, and TiB₂ were developed and evaluated for their neutron shielding performance. Monte Carlo simulations using the GEANT4 code and experimental measurements showed that neutron attenuation efficiency strongly depends on the filler composition and material density. The background radiation dose of 1.4280 µSv/h was used as a reference for calculating the radiation protection efficiency (RPE).

Among the reference materials, paraffin, ordinary concrete (OC), and hematite–serpentine concrete (H-SC) exhibited RPE values of 30.18%, 21.76%, and 20.82%, respectively. In contrast, epoxy–ceramic hybrid composites (CS1–CS4) displayed higher efficiencies, ranging from 38.10% to 40.60%, confirming their superior shielding capability. The CS3 sample, containing 26% NiO, 9% TiB₂, and 7% FeB with a density of 4.51 g/cm³, showed the best performance due to the synergistic effects of high atomic number oxides and boron-rich phases.

Overall, increasing NiO, TiB₂, and FeB contents while optimizing density significantly improved neutron absorption and scattering. The combination of boron-based compounds and transition-metal oxides provided a dual mechanism for fast-neutron moderation and thermal-neutron capture. These results suggest that the developed epoxy–metal oxide–boron composites are promising lightweight materials for shielding against neutron and gamma radiation in nuclear reactors, radiation facilities, and aerospace systems.

Keywords: Neutron, composite, Geant4.

Received: 14.10.2025

Revised: 17.12.2025

Accepted: 25.12.2025

*Corresponding author: Bünyamin AYGÜN, PhD
Department of Electronics and Automation, Vocational School,
Agri Ibrahim Cecen University, Agri Turkey
E-mail: baygun@agri.edu.tr

Cite this article as: B. Aygün, Development and Evaluation of Epoxy-Based Composites Containing NiO, Cr₂O₃, MnO₂, FeB and TiB₂ for Enhanced Neutron Shielding Performance, *Eastern Anatolian Journal of Science*, Vol. 11, Issue 1-2, 9-16, 2025.

1. Introduction

Neutron radiation is a unique form of non-directly ionizing radiation generated during nuclear fission, fusion, and spallation reactions. Unlike charged particles such as protons or electrons, neutrons lack an electric charge, enabling them to deeply penetrate matter and interact with atomic nuclei. These interactions may induce transmutation reactions, generate secondary ionizing radiation such as gamma rays, or form radioactive nuclides (Yue et al. 2013). Owing to these characteristics, neutron radiation is extensively applied in nuclear power generation, neutron diffraction and scattering experiments, materials characterization, cosmology, oil and mineral exploration, and advanced medical treatments, including Boron Neutron Capture Therapy (BNCT). However, due to their high penetration depth and secondary radiation production, neutrons present one of the most significant hazards to workers, patients, and operators if not adequately shielded (Nouraddini-Shahabadi et al., 2024).

Compared to gamma, alpha, or beta radiation, shielding against neutrons is more complex. While charged particles are easily attenuated by dense materials, neutrons require a combination of hydrogen-rich moderators to slow them to thermal energies and absorbers with high capture cross-sections, such as ¹⁰B, ⁶Li, or ¹⁵⁷Gd, to capture thermalized neutrons. Furthermore, careful design is needed to minimize secondary gamma emission following neutron capture, which can otherwise compromise overall protection efficiency. Therefore, the development of effective, multifunctional shielding materials remains an ongoing challenge.

A wide variety of neutron shielding materials have been investigated. Conventional approaches include heavy concretes (Aygün et al., 2018), lead- and steel-based shields, and alloys with high-Z elements (Qi et al., 2022; Oh et al., 2024; Aygün et al., 2022). For

instance, stainless steels (316LN, 304L) and high-entropy alloys such as CoNiFeCrTi have been studied for combined strength and radiation attenuation (Sakar et al., 2023). Aluminum and titanium alloys are frequently used in aerospace because of their low weight, but their poor neutron absorption requires modification through fillers or coatings (Sukumaran et al., 2024). Glass systems doped with oxides of boron, gadolinium, or rare-earth elements also show promise, but their brittleness and fabrication challenges limit practical applications (Kaewkhao et al., 2018; Alajerami et al., 2024; Ekinici et al., 2024).

In recent years, polymer-based composites have attracted increasing attention. Polymers such as epoxy, polyethylene, and polypropylene are lightweight and easy to process. Polymers with high hydrogen content can provide significant neutron absorption. By adding fillers such as boron or lithium to these polymers, high-performance neutron absorbers can be obtained (Aygün et al., 2020).

Borate minerals such as ulexite, tincal, and colemanite have been incorporated into polymer matrices to produce polypropylene composites, and samples rich in colemanite were shown to exhibit superior neutron absorption (Bilici et al., 2021). To further enhance the radiation-absorbing capability of polymers, composite materials were produced by adding lithium fluoride (LiF), NiO, and Cr₂O₃ into epoxy and coating them with sodium silicate; this improved both neutron absorption and thermal resistance properties (Aygün et al., 2020).

Polymers enriched with tungsten and boron compounds can also be used in radiation shielding. Epoxy composites containing tungsten carbide (WC) and boron nitride (BN) were designed, and those with high filler contents demonstrated good structural strength and neutron attenuation capacity (Kaya et al., 2025). As an innovative approach in the development of radiation-shielding materials, gadolinium oxide–epoxy composites containing 10 wt% Gd₂O₃ were developed, which significantly reduced both fast and thermal neutron flux (Safavi et al., 2024), while epoxy–graphene hybrids (Benedetti et al., 2025) provided multifunctionality for shielding, thermal, and mechanical applications.

For space radiation shielding, polymer-based systems enhanced with carbon derivatives, boron nitride (BN), lithium borates, and rare-earth oxides are gaining increasing importance (Toto et al., 2024). Despite

these advances in composite technology, several challenges remain. Many polymer composite materials suffer from filler dispersion problems, reduced mechanical strength at high filler loadings, and increased density when heavy oxides are added. To overcome these issues, polymer–ceramic hybrid systems combining hydrogen-rich matrices with multifunctional fillers are being designed.

Boron-containing compounds (e.g., carboranes, borophosphates, B₄C) and lithium salts (Li₂B₄O₇, LiF) can efficiently capture neutrons with minimal gamma emission. Components such as BN and hBN improve the composite’s heat transfer and mechanical stability while reducing thermal stress accumulation. Transition-metal oxides such as NiO and Cr₂O₃ enhance both gamma and neutron attenuation while improving mechanical strength and reducing density.

In this study, four new multifunctional epoxy-based composites (CS1–CS4) reinforced with NiO, Cr₂O₃, MnO₂, FeB, and TiB₂ fillers were designed. The compositions were optimized to balance neutron absorption, thermal and mechanical strength, and weight reduction. Theoretical neutron-shielding parameters—macroscopic removal cross-section (Σ_R), half-value layer (HVL), mean free path (MFP), and radiation protection efficiency (RPE)—were determined using Monte Carlo simulations (GEANT4). The composites were compared with conventional materials such as paraffin, ordinary concrete (OC), and hematite–serpentine concrete (H-SC). These newly developed composite materials show potential for next-generation neutron shielding in nuclear reactors, medical radiation facilities, radioactive-waste storage areas, and aerospace systems.

Neutron attenuation principles

The macroscopic cross section (Σ) combines the microscopic probability of neutron interaction (σ) with the number density of atoms (N) in a material. It is a fundamental parameter in neutron transport, shielding design, and reactor physics because it quantifies how strongly a bulk material attenuates or interacts with neutrons.

The macroscopic cross section is given by the formula:

$$\Sigma = (\rho / A) \times N_a \quad (1)$$

Where, Σ : Macroscopic cross section (cm⁻¹), ρ :

Density of absorber material, A : Molecular weight of absorber (g/mol) material, N_a : Avogadro’s number (6.022 × 10²³ atoms/mol)

The number of atoms per unit volume (N) describes how many atoms are present in one cubic centimeter of

a material. The number of atoms per unit volume (N) represents how many atoms are packed into a unit of space (atoms/cm³). It is determined by the material's density and atomic weight, and it directly influences how effectively the material can interact with and attenuate neutrons. It is also called atomic number density. This value is crucial because the probability of a neutron interacting with matter depends directly on how many atoms it encounters along its path (Khayatt et al., 2010).

$$N = (\rho / A) \times N_0 \quad (2)$$

where N_0 is Avogadro's number.

The removal cross section (ΣR) quantifies the ability of a material to attenuate fast neutrons by removing them from the beam (via scattering, absorption, or capture). It is essential for calculating shielding thickness, HVL, mean free path, and designing neutron protection systems.

$$\Sigma R = \Sigma (\Sigma R/\rho)_i \times \rho_i \quad (3)$$

$$\rho_i = w_i \times \rho \quad (4)$$

where: w_i : Weight fraction of i -th component ρ_i : Partial density.

The Half Value Layer (HVL) is the thickness of a shielding material that reduces neutron (or any radiation) intensity by half. It depends on the removal cross section (ΣR), and materials with higher ΣR values have smaller HVL, making them better neutron shields.

$$HVL = \ln(2) / \Sigma R \quad (5)$$

HVL represents the thickness of material required to reduce neutron intensity by half.

The Mean Free Path (λ) is the average distance a neutron travels before interacting in a material. It is inversely proportional to the removal cross-section and provides a direct measure of shielding effectiveness. A short λ indicates strong shielding capacity, whereas a long λ denotes weak shielding performance of the sample.

$$\lambda = 1 / \Sigma R \quad (6)$$

It is the average distance a neutron travels before an interaction.

The Neutron Transmission Factor (NTF) is the ratio of transmitted to incident neutron intensity. It is a direct measure of how effective a material is at reducing neutron flux the lower the NTF, the better the shielding.

$$NTF = I / I_0 \quad (7)$$

where: I , Transmitted neutron intensity I_0 , Incident neutron intensity

The Radiation Protection Efficiency (RPE) is a percentage indicator of shielding performance.

It is complementary to the transmission factor (NTF), with higher RPE meaning stronger protection. RPE is widely used in shielding design, safety analysis, and comparative studies of neutron-absorbing materials.

$$RPE = (1 - N / N_0) \times 100\% \quad (8)$$

where: N , neutron dose transmitted through the shield. N_0 , Incident neutron dose

2. Materials and Methods

3.1. Monte Carlo simulation code GEANT4

Geant4 (Geometry and Tracking version 4) is an open-source C++ software toolkit developed by an international collaboration led by CERN. It is used to simulate the passage of particles through matter. Geant4 is widely applied in high-energy physics, medical physics, radiation protection, nuclear engineering, and space science. Geometry and Materials, supports complex 3D geometries and user-defined composite materials. For Epoxy-BN-borophosphate composites, Geant4 allows the modeling of epoxy resin mixed with NiO, Cr₂O₃, Li₂B₄O₇, BN-carborane hybrid, and borophosphate microspheres. Simulations can be used to study gamma attenuation, neutron moderation and absorption, as well as energy deposition. Different composite designs (CS1-CS4) can be compared in terms of shielding performance, thermal neutron capture efficiency, and secondary radiation yields (Wellisch, 2005). Geant4 simulation geometry is given in Figure 1.

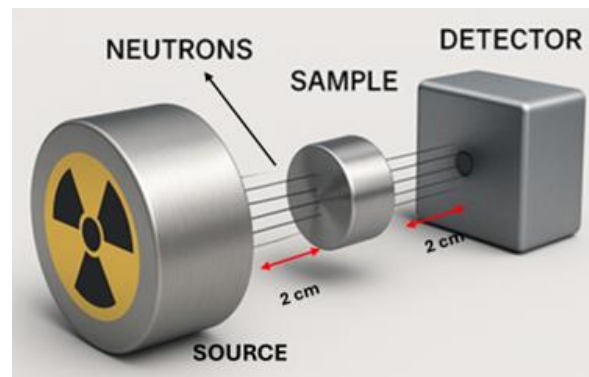


Figure 1. Geant4 simulation geometry Geant4 3D visual

3.2. Sample preparation and experimental

Weigh all dry powders Manganese oxide (MnO₂), Nickel oxide (NiO), Chromium(III) oxide (Cr₂O₃), Ferroboron (FeB), and Titanium diboride (TiB₂) according to the design composition. Add the powders gradually to the epoxy resin while stirring. Use a laboratory blender or mechanical stirrer to homogenize the mixture for 20 minutes. After obtaining a uniform mixture, allow the composite paste to rest and degas

for 20 minutes. Pour the homogenized mixture into the prepared molds (with release agent applied) on the vacuum de-air (20–30 kPa absolute, 1–2 min). Level the surface and remove visible air bubbles. Before all samples were cured 2–4 h at 23–25 °C, then 2 h at 60 °C and 2 h at 80 °C. Demold, cool, and machine to the final size (1 cm thickness). The chemical compositions of these composite samples are detailed in Table 1, and the produced sample images are presented in Figure. 2.

Table 1. Chemical composition ratios and density of composite samples (CS) (%)

Sample Code	CS1 ($\rho = 4.21$ g/cm ³)	CS2 ($\rho = 4.20$ g/cm ³)	CS3 ($\rho = 4.51$ g/cm ³)	CS4 ($\rho = 4.21$ g/cm ³)
Epoxy Resin (%)	30	30	30	30
NiO (%)	20	23	26	29
Cr ₂ O ₃ (%)	30	25	20	15
MnO ₂ (%)	12	10	14	6
FeB (%)	3	5	7	9
TiB ₂ (%)	5	7	9	11

CS: Composite sample

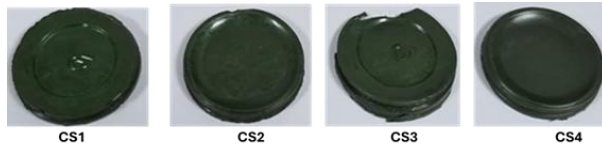


Figure. 2. Produced composite samples

In the dose measurement experiments, a point-type Am–Be fast neutron source was employed in conjunction with a BF₃ neutron detector. The experimental setup, illustrated in Figure 3, was specifically designed to perform absorption measurements. Initially, the background dose (D_0), representing the unattenuated neutron dose emitted directly from the source, was measured. Subsequently, each composite sample was positioned between the source and the detector and exposed to neutron radiation, enabling the absorbed dose detected (D_D) to be recorded. Finally, the dose absorbed by the sample (D_S) was calculated according to the relation: $D_S = D_0 - D_D$.

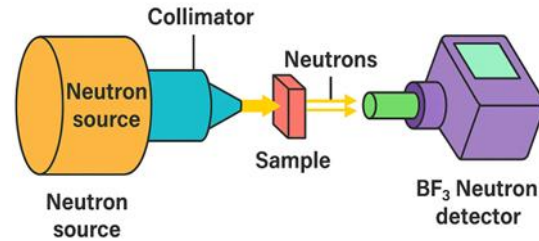


Figure 3. Neutron equivalent dose rate measurement system

4. Results and discussion

In the current work, samples CS1 through CS4 explore an epoxy matrix reinforced with varying amounts of NiO, Cr₂O₃, MnO₂, FeB, and TiB₂, targeting an optimum balance between mechanical stability and neutron attenuation capability. The strategy of combining boron-bearing phases (FeB, TiB₂) with high-Z oxides (NiO, Cr₂O₃, MnO₂) mirrors approaches in polymer-based shielding composites where neutron moderators and absorbers are integrated (Safavi et al., 2024). For instance, Safavi et al. (2024) used Gd₂O₃–epoxy systems and demonstrated strong neutron attenuation at modest filler contents (0.5–10 wt%). In comparison, these composites use a more diversified filler palette to achieve both moderation (via lighter elements) and absorption/scattering (via heavier oxides). Among the samples, CS3 (density ≈ 4.51 g/cm³) is likely to show superior fast-neutron attenuation given its increased overall mass per unit volume; higher density favors elastic and inelastic scattering interactions, thereby increasing the probability of energy loss per unit thickness (Yassin & Alzahrani, 2021). However, for effective thermal neutron absorption, the presence, distribution, and isotopic composition of boron in FeB and TiB₂ become critical. Previous studies on TiB₂-based boron composites have found that adding boron phases can yield modest shielding rates (e.g., $\sim 17.5\%$ for thermal neutrons), but that performance strongly depends on filler dispersion and composite homogeneity (TiB₂–Al Composite Study, 2021). Likewise, Bilici et al. (2021) investigated epoxy composites doped with metal oxides and found that while oxide additions improve gamma and fast-neutron scattering, the benefit for slow-neutron capture is limited unless a high-cross-section absorber is incorporated.

Thus, in comparing these composites to existing epoxy shielding materials:

Fast-neutron shielding: The densest formulation (especially CS3) is promising, since the combination of heavy oxides and boron phases can slow down and scatter fast neutrons before capture. This is consistent

Sample code	Mean Free Path (mm)	Half Value Layer (cm)	Transmission Factor	Effective Removal Cross Section (cm ⁻¹)
Paraffin	4.88 ± 0.047	3.384 ± 0.038	0.81476	0.2048
OC	5.98 ± 0.056	4.147 ± 0.041	0.84605	0.1671
H-SC	6.42 ± 0.062	4.451 ± 0.045	0.85581	0.1557
CS1	3.28 ± 0.031	2.274 ± 0.022	0.73729	0.3047
CS2	3.30 ± 0.030	2.290 ± 0.029	0.73883	0.3026
CS3	2.95 ± 0.021	2.049 ± 0.024	0.71309	0.3381
CS4	3.25 ± 0.025	2.259 ± 0.025	0.73577	0.3068

with the known principle that heavier nuclei help with inelastic scattering (Jia et al., 2021; Yassin & Alzahrani, 2021). Thermal/epithermal neutron capture: The efficacy will hinge on boron content, isotopic enrichment (¹⁰B), and dispersion of FeB/TiB₂ phases. Compared to pure Gd₂O₃ fillers, which exhibit extremely high neutron absorption cross sections (Safavi et al., 2024), this system may underperform in capture efficiency but might mitigate this by better mechanical performance or broader energy-range attenuation.

4.1. Neutron absorption parameters

It is, of course, likely that there are differences between experimental measurements and simulation results. This arises because in simulation studies, the material is assumed to be perfectly homogeneous and the geometry is modeled with exact dimensions, while in experimental practice neither absolute homogeneity nor flawless geometric precision can be achieved. Small deviations and imperfections in processing or dispersion may alter shielding responses. A margin of error of up to 10% between simulations and experiments is typically considered acceptable (Kurt et al., 2020). Nevertheless, when the shielding capacity of a material is well-predicted in simulations, experimental verification often produces consistent outcomes. This highlights the critical role of simulation-based design in radiation shielding research. With powerful tools such as Geant4, essential shielding parameters—including the effective removal cross-section (Σ_R), mean free path (λ), half-value layer (HVL), and radiation protection efficiency (RPE)—can be predicted prior to production, guiding experimental design and reducing costly trial-and-

error (Yassin & Alzahrani, 2021). In this study, such an approach was adopted: production strategies for CS1–CS4 were based on Geant4 simulation outcomes and then validated experimentally. The close alignment of theoretical and experimental values across most formulations supports the conclusion that combining boron-rich reinforcements (FeB, TiB₂) with high-density oxides (NiO, Cr₂O₃, MnO₂) provides an effective pathway to develop composites with predictable neutron shielding properties (Bilici et al., 2021; Safavi et al., 2024).

Table 2 Comparison of shielding parameters in 1 cm thick samples for 10⁵ incident fast neutrons (4.5 MeV)

P: Paraffin, OC: Ordinary concrete, H-SC: hematite-serpentine concrete, CS: Composite sample

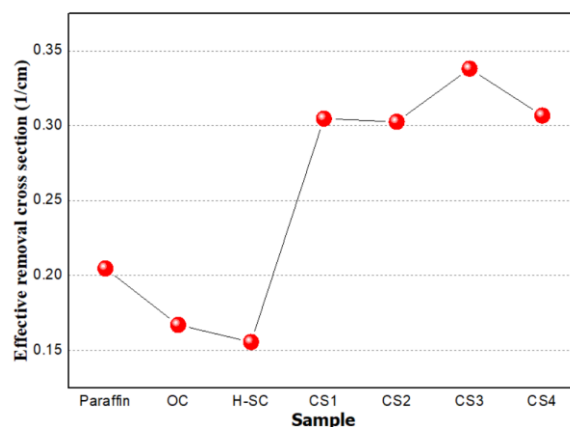


Figure 4. Effective removal Cross Section (cm⁻¹) comparison of samples

According to the data presented in Tables 1 and 2, the fast neutron shielding performance of the composite samples was evaluated using the parameters Mean Free Path (MFP), Half Value Layer (HVL), and Transmission Factor (TF). The results consistently show that the shielding efficiency follows the order CS3 > CS4 > CS1 ≈ CS2 >> Paraffin > OC > H-SC, indicating a strong correlation among all parameters. Among all the samples, CS3 exhibited the most effective shielding performance, with the lowest MFP (2.95 mm) and HVL (2.05 cm) values, as well as the smallest TF (0.7131). This superior behavior is attributed to its high contents of NiO (26%), TiB₂ (9%), and FeB (7%), combined with a high density of

Sample code	Absorbed Dose by Samples ($\mu\text{Sv/h}$)	Radiation protection efficiency (%)
Background	1.4280	
Paraffin	0.4309 \pm 0.043	30.18
OC	0.3107 \pm 0.030	21.76
H-SC	0.2973 \pm 0.028	20.82
CS1	0.5533 \pm 0.051	38.75
CS2	0.5440 \pm 0.053	38.10
CS3	57.970 \pm 0.058	40.60
CS4	0.5563 \pm 0.055	38.96

4.51 g/cm³. The presence of Ni and Ti, which possess high atomic numbers, increases the probability of neutron scattering and absorption, while boron-containing compounds such as FeB and TiB₂ effectively moderate fast neutrons by capturing them and reducing their energy. Furthermore, the reduced Cr₂O₃ content in CS3 positively influenced the overall neutron interaction probability, since Cr₂O₃ has a relatively low neutron absorption cross section.

In comparison, CS4, although containing higher proportions of NiO (29%) and TiB₂ (11%), demonstrated slightly lower shielding performance than CS3 due to its reduced MnO₂ (6%) content, which limited its neutron slowing capability. CS1 and CS2 showed balanced yet moderate shielding efficiencies because of their intermediate ratios of NiO, Cr₂O₃, and TiB₂. Their relatively lower densities (4.20–4.21 g/cm³) also restricted the neutron interaction probability within these samples. The reference materials, Paraffin, OC, and H-SC, exhibited considerably lower neutron shielding capabilities. Among them, H-SC (MFP: 6.42 mm, HVL: 4.45 cm, TF: 0.8558) showed the weakest performance, while OC and Paraffin, although hydrogen-rich, were only moderately effective in slowing down neutrons and lacked heavy elements necessary for efficient absorption.

In conclusion, both experimental parameters and compositional properties clearly indicate that the increase in NiO, TiB₂, and FeB contents, along with higher material density, substantially enhances the neutron attenuation efficiency of the composites. In this context, CS3 demonstrated the most effective fast neutron shielding performance among all the samples, followed by CS4, CS1, and CS2. Paraffin, OC, and H-SC served as reference materials, exhibiting the weakest attenuation performance due to their low densities and light-element compositions.

4.2. Neutron absorption dose results

Table 3 Absorbed dose results of all samples

P: Paraffin, OC: Ordinary concrete, H-SC: hematite-serpentine concrete, CS: Composite sample

Figure 4. Radiation protection efficiency (%)

When Table 3 and Figure 4 are carefully examined, the background dose emitted by the radiation source is recorded as 1.4280 $\mu\text{Sv/h}$. According to this dose level, the protection efficiencies of the reference materials are as follows: paraffin 30.18%, ordinary concrete (OC) 21.76%, and hematite-serpentine concrete (H-SC) 20.82%. The composite CS series clearly exceeds these values, with CS1 38.75%, CS2 38.10%, CS3 40.60%, and CS4 38.96%. Therefore, based on both the table and the graph, the general efficiency ranking is CS3 > CS4 \approx CS1 \approx CS2 > Paraffin > OC > H-SC, and the best overall performance belongs to CS3. CS3 has the highest density at 4.51 g/cm³, and its composition contains increased proportions of NiO, FeB, and TiB₂. This combination suggests a performance trend consistent with the high efficiency observed in CS3. In CS4, the amounts of NiO, FeB, and TiB₂ are even higher, yet the density decreases to 4.21 g/cm³. This implies good absorption potential in mixed radiation fields particularly those containing a neutron component while the photon-shielding benefit may not be as strong as that of CS3. Across the sequence CS1 \rightarrow CS4, Cr₂O₃ and MnO₂ decrease, whereas NiO, FeB, and TiB₂ increase. High-atomic-number oxides (especially NiO) enhance photon interaction cross-sections, while the boron-containing phases (FeB, TiB₂) strengthen neutron-capture ability. Considering this composition–density relationship, CS3 can be identified as the most balanced and high-performance candidate, whereas CS4 appears to be comparatively more advantageous against neutron radiation.

5. Conclusions

In this study, epoxy-based multifunctional composites containing NiO, Cr₂O₃, MnO₂, FeB, and TiB₂ were successfully synthesized and evaluated in terms of their neutron shielding capabilities. Both Monte Carlo simulation (GEANT4) and experimental measurements clearly demonstrated that neutron attenuation performance depends strongly on the filler composition and material density. The background

radiation dose of 1.4280 $\mu\text{Sv/h}$ was used as a reference for evaluating the radiation protection efficiency of all samples. Among the reference materials, paraffin, ordinary concrete (OC), and hematite–serpentine concrete (H-SC) exhibited moderate protection efficiencies of 30.18%, 21.76%, and 20.82%, respectively. In contrast, the composite series (CS1–CS4) showed significantly higher values—38.75%, 38.10%, 40.60%, and 38.96%—confirming that polymer–ceramic hybrid structures provide superior neutron attenuation compared with conventional materials. The CS3 sample, which contains 26% NiO, 9% TiB₂, and 7% FeB and has a density of 4.51 g/cm³, exhibited the best absorption performance owing to the synergistic effects of high atomic number oxides and boron-rich phases. Furthermore, compositional analysis clearly indicates that CS3, having the highest density (4.51 g/cm³) and enriched contents of NiO, FeB, and TiB₂, possesses superior radiation-shielding ability compared to the other samples. Although CS4 contains a higher boron content, its slightly lower density suggests that it may perform better in mixed radiation environments where neutron moderation dominates, whereas CS3 remains the most balanced and effective candidate for combined neutron and photon attenuation. Overall, the results show that increasing the fractions of NiO, TiB₂, and FeB while optimizing matrix density significantly enhances neutron absorption and scattering probabilities. The integration of boron-based phases for neutron capture establishes a synergistic mechanism leading to high Radiation Protection Efficiency (RPE) values. Therefore, the developed composites offer promising alternatives to conventional shielding materials for applications in nuclear reactor components, radiation laboratories, and aerospace protection systems.

Acknowledgement

This study was supported by the Scientific and Technological Research Council of Ağrı İbrahim Çeçen University (BAP) with MYO.24.003 code.

References

YUE, A. T., DEWEY, M. S., GILLIAM, D. M., GREENE, G. L., LAPTEV, A. B., NICO, J. S., SNOW, W. M., WIETFELDT, F. E. (2013). Improved determination of the neutron lifetime. *Physical Review Letters*, 111(22), 222501.

- ALAJERAMİ, Y.S.M., MHAREB, M.H.A., SAYYED, M.I., HAMAD, M.KH., ABUELHIA, E. A. A., ALQAHTANI, M. Y., IMHEIDAT, M. A. (2024). Physical and radiation shielding properties for borate, borotellurite, and tellurite glass system modified with different modifiers: Comparative study, *Optical Materials*, 147, 114558.
- AYGÜN, B. (2020). Developed and Produced New Laterite Refractory Brick Samples Protective for Gamma and Neutron Radiation Using GEANT4 Code. *Gümüşhane Üniversitesi Fen Bilimleri Dergisi*, 10(1), 1-6.
- AYGÜN, B., & KARABULUT, A. (2018). Development and Production of High Heat Resistant Heavy Concrete Shielding Materials for Neutron and Gamma Radiation. *Eastern Anatolian Journal of Science*, 4(2), 24-30.
- AYGÜN, B., & KARABULUT, A. (2022). Investigation of epithermal and fast neutron shielding properties of Some High Entropy Alloys Containing Ti, Hf, Nb, and Zr. *Eastern Anatolian Journal of Science*, 8(2), 37-44.
- NESLİHAN, E., NORAH, A.M.A., KHATTARİ, Z.Y., RAMMAH, Y.S., AYGÜN, B., KURUCU, Y., SARITAŞ, S. (2024). Evaluation of lithium tetra borate glass-ceramics: Structural, physical and radiation safety properties using experimental and theoretical methods, *Nuclear Engineering and Technology*, 56, 11, 4887-4894.
- BENEDETTI, L., ORİKASA, K., ALEMAN, A., JOHN, D., AGARWAL, A. (2025). Enhancing polymer composites: The impact of three-dimensional nanomaterial architectures on thermal, electrical, and radiation shielding properties. *Composites Part A: Applied Science and Manufacturing*. 198, 109110.
- AYGÜN, B., ŞAKAR, E., SINGH, V. P., SAYYED, M. I., KORKUT, T., & KARABULUT, A. (2020). Experimental and Monte Carlo simulation study on potential new composite materials to moderate neutron-gamma radiation. *Progress in Nuclear Energy*, 130.
- BILICI, İ., AYGÜN, B., DENİZ, C. U., ÖZ, B., SAYYED, M. I., & KARABULUT, A. (2021). Fabrication of novel neutron shielding materials: Polypropylene composites

- containing colemanite, tincal and ulexite. *Progress in Nuclear Energy*, 141.
- EL-KHAYATT, A.M. (2010). Calculation of fast neutron removal cross-sections for some compounds and materials. *Annals of Nuclear Energy*. 37,2, 218-222.
- KAEWKHAO, J., KORKUT, T., KORKUT, H., AYGÜN, B., YASAKA, P., TUSCHAROEN, S., INSİRİPONG S., A. KARABULUT.(2017). Monte Carlo Design and Experiments on the Neutron Shielding Performances of B₂O₃-ZnO-Bi₂O₃ Glass System. *Glass Phys Chem* 43, 560-563.
- KAYA, N., KARAMAN, M. & AKSOY, R. (2025). Structural, Mechanical, and Radiation Shielding Properties of Epoxy Composites Reinforced with Tungsten Carbide and Hexagonal Boron Nitride. *J Inorg Organomet Polym*.
- NOURADDINI-SHAHABADI, A., REZAIE, M.R., HIEDARIZADEH, Y. SAEED, M. (2024). Monte Carlo simulation and practical investigation of body organs activation by Am-Be neutron source. *J. Korean Phys. Soc.* 84, 672-680.
- QI Z, YANG Z, LI J, GUO Y, YANG G, YU Y, ZHANG J (2022). The Advancement of Neutron-Shielding Materials for the Transportation and Storage of Spent Nuclear Fuel. *Materials*. 15(9),3255.
- SAKAR, E., GULER, O., ALIM, B., SAY, Y., & DIKICI, B. (2023). A comprehensive study on structural properties, photon and particle attenuation competence of CoNiFeCr-Ti/Al high entropy alloys (HEAs). *Journal of Alloys and Compounds*, 931.
- TOTO, E., LAMBERTINI, L., LAURENZI, S., SANTONICOLA, M.G. (2024). Recent Advances and Challenges in Polymer-Based Materials for Space Radiation Shielding. *Polymers* 16, 382.
- SUKUMARAN, A. K., ZHANG, C., RENGIFO, S., RENFRO, M., GARINO, G., SCOTT, W., ... AGARWAL, A. (2024). Tribological and radiation shielding response of novel titanium-boron nitride coatings for lunar structural components. *Surface and Coatings Technology*, 476.
- BILICI, H., KORKUT, T., KARABULUT, A., & DEMIR, N. (2021). Radiation shielding and mechanical properties of epoxy composites containing different metal oxides. *Radiation Physics and Chemistry*, 188, 109642.
- JIA, X., CHEN, H., LI, Y., & WANG, Z. (2021). Neutron shielding and mechanical properties of short carbon fiber reinforced aluminium 6061-boron carbide hybrid composite. *Ceramics International*, 47 (7), 10193-10196.
- SAFAVI, A., FARAJI, M., & RAMEZANI, S. (2024). Development of epoxy-Gd₂O₃ nanocomposites for neutron and gamma radiation shielding. *Journal of Applied Polymer Science*, 141(12), 54028.
- KURT, B., TURHAN, M. F., YALÇINKAYA, S., & DEMIR, N. (2020). Investigation of neutron shielding performances of various materials using the Geant4 simulation code. *Radiation Physics and Chemistry*, 176, 109072.
- YASSIN, A. M., & ALZHRANI, B. (2021). A review on neutron shielding materials: Development and applications. *Journal of Nanomaterials*, 5541047.